**Technical Paper**

Journal of the Society of
Naval Architects of Korea
Vol. 20, No. 2, June 1983

# The Added Mass and Damping Coefficients of and the Excitation Forces on Four Axisymmetric Ocean Platforms

by

Kwang June Bai*

## Abstract

This paper presents numerical results of the added mass and damping coefficients of vertical axisymmetric bodies on or under the free surface. Also computed are the excitation forces on these bodies due to an incident regular wave system. The numerical scheme employs a localized finite-element method, which is based on the theory of the calculus of variations. The excitation forces and moments on a submerged half-spheroid lying on the bottom are computed and compared with the results obtained by others. The agreement is good. Several specific types of floating vertical axisymmetric platforms are considered for ten different wave lengths, in connection with the design of an ocean-thermal-energy converter platform. The added mass and damping coefficients, as well as the excitations, are presented. It is shown that simple strip theory gives a good approximation of the sway (and pitch) added mass for a disc platform having a long circular cylinder.

## 1. Introduction

Small oscillatory motions of an inviscid, incompressible fluid with a free surface are described by a boundary value problem governed by Laplace's equation with a mixed boundary condition on the free surface, a homogeneous Neumann condition on the bottom of the fluid, and an appropriate radiation condition at infinity. Forced motion or diffraction problems of a floating or submerged body require an additional boundary condition on the body surface as well, generally stating that the normal velocity of the body and fluid are equal.

When we restrict the body geometry to be a body of revolution with a generator parallel to the direction of the gravity force, the general three-dimensional problem reduces to a far simpler set of two-dimensional problems. For this specific type of body geometry, the added mass and damping forces con tain only nine non-zero elements in the general $6\times6$ matrices. Further, there are only four elements to compute out of nine non-zero elements due to symmetry.

The present numerical method was previously used with success by the present author. [1, 2, 3] Details on this numerical method are not given in this paper, since one can find them in the above references.

A diffraction problem for a submerged half-spheroid lying on the bottom is treated. The excitation forces and moments are compared with the results obtained by Rao and Garrison. [4] Agreement is good.

Manuscript received: May 12, 1983

* Member, DTNSRDC; Presently Visiting Professor at Seoul National University

Also treated are four configurations of flating platforms. These specific geometries are considered in the design of a thermal-energy converter floating in the ocean. Both forced-motion and diffraction problems are solved for the four platforms over a wide range of realistic wave lengths, from approximately 50 feet up to 5000 feet.

For the disc platform with a long pipe having a closed end our numerical results for sway and pitch added mass and moment are compared with those computed from simple strip theory, which is strictly two-dimensional. Agreement is good for all the wave lengths considered here. It is of interest to note that the sway and pitch added mass of this specific platform stay nearly constant for various wave lengths. The same geometry is also considered with the end of pipe open, for the case of the heave forced-motion problem,in order to test the difference in the added masses, for the two different conditions at the end of the pipe. A simplified mathematical model related to this model is also considered in the heave forced-motion problem by assuming the attached pipe is infinitely long with an open end. For all three models, the added masses and pitch moments are compared.

As a test of these numerical results, the exciting forces are also computed from the Haskind relations by using the results of the forced motion problem. Agreement is very good. Newman [5] shows that the phase of the sway exciting force and of the pitch exciting moment are the same. Our numerical computations of phase are in good agreement with Newman's phase relation.

All of the results for the excitation forces and moments presented here are obtained by solving the diffraction problems.

## 2. Formulation of the problem

We consider here the wave-body interaction of an axisymmetric body floating in or submerged under a free surface. Such interaction may occur either as a forced motion problem or as a diffraction problem. In the former case, the wave motion is generated

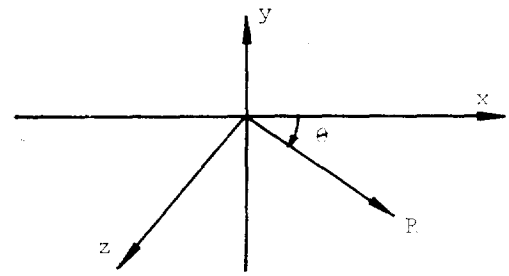


**Fig. 1** Coordinate System

by some prescribed motion of the body; in the latter, the body is held fixed but subject to the excitation force due to an incident wave system. It is well known that mathematically, these two problems are essentially identical, the only difference being that the boundary condition on the body takes different functional specifications.

We assume that the body has no forward translation velocity, the fluid is incompressible and inviscid, and the flow irrotational. A linearized free-surface boundary condition will be used. It is convenient to introduce a cylindrical $(R\theta y)$ coordinate system, with the y-axis pointing vertically upwards and the $R\theta$ plane in the undisturbed free surface. The R-axis coincides with the x-axis when $\theta$ is zero and with the z-axis when $\theta$ is $\pi/2$ as shown in Figure 1, where the xyz coordinate system is rectangular and right-handed.

Periodic oscillatory flow is described by the velocity potential

$$\Phi(R,\theta,y,t)=Re\ \{\phi(R,\theta,y)\ e^{-\sigma t}\} \tag{2.1}$$

where $\sigma$ is the frequency and $\phi(R,\theta,y)$ is a complex spatial velocity potential, which must satisfy

$$\frac{1}{R}\frac{\partial}{\partial R}\left(R\frac{\partial\phi}{\partial R}\right)+\frac{1}{R^2}\frac{\partial^2\phi}{\partial\theta^2}+\frac{\partial^2\phi}{\partial y^2}=0 \tag{2.2}$$

in the fluid. As the boundary conditions, we have

$$\phi_y-\nu\phi=1 \quad \text{on } y=0 \tag{2.3}$$

$$\phi_n=V_n \quad \text{on the body} \tag{2.4}$$

$$\phi_n=0 \quad \text{on the bottom } (y=-h) \text{ or } y\to-\infty \text{ (for infinite depth)} \tag{2.5}$$

$$\lim_{R\to\infty}\sqrt{R}\,(\phi_R-im_0\phi)=0 \tag{2.6}$$

where $\nu=\frac{\sigma^2}{g}$ and the wave number $m_0$ is determined from

$$\nu=m_0 \tanh m_0 h \tag{2.7}$$

When we consider an axisymmetric body whose axis coincides with the y-axis, then the potential $\phi$ can be assumed to have a form

$$\phi(R,\theta,y)=\sum_{k=0}^{\infty}\varphi^{(k)}(R,y)\cos(k\theta+\beta) \tag{2.8}$$

Similarly, the normal velocity on the body can be expressed as

$$V_n=\sum_{k=0}^{\infty}v_n^{(k)}\cos(k\theta+\beta) \tag{2.9}$$

Here $\varphi^{(k)}(R,y)$ and $v^{(k)}(R,y)$ are functions of only $R$ and $y$, and $\beta$ is an arbitrary phase angle. Without loss of generality the phase angle $\beta$ will be taken to be zero here.

By substituting (2.8) and (2.9), into equations (2.2) through (2.6), for $k=0,1,2$, we have

$$-\frac{1}{R}\frac{\partial}{\partial R}\left(R\frac{\partial\varphi^{(k)}}{\partial R}\right)-\frac{k^2}{R^2}\varphi^{(k)}+\varphi_{yy}^{(k)}=0\begin{cases}0\le R\\ -h\le y\le 0\end{cases} \tag{2.10}$$

$$\varphi_y^{(k)}-\nu\varphi^{(k)}=0,\quad \text{at } y=0 \tag{2.11}$$

$$\varphi_n^{(k)}=v_n^{(k)} \qquad \text{on } S_0 \tag{2.12}$$

$$\varphi_n^{(k)}=0 \qquad \text{on } y=-h \tag{2.13}$$

$$\lim_{R\to\infty}\sqrt{R}\left(\varphi_R^{(k)}-im_0\varphi^{(k)}\right)=0 \tag{2.14}$$

It should be noted that the reduced problem given in (2.10) through (2.14) is defined only in two dimensions, i.e., in the Ry-plane ($R\ge 0$).

In the forced motion problem, we considered heave, surge and pitch motions which by symmetry are sufficient to describe the complete six degrees-of-freedom problem of an axisymmetric body. It suffices to solve the above equations, (2.10) through (2.14), for $k=0$ for heave motion, and for $k=1$ for surge and pitch motions. For unit-velocity rigid-body motions, the normal velocity on the body boundary $S_0$ is expressed as

$$v_n^{(0)}=n_2 \tag{2.15}$$

for heave motion

$$v_n^{(1)}=n_1 \tag{2.16}$$

for surge motion, and

$$v_n^{(1)}=\vec{r}\times\vec{n} \tag{2.17}$$

for pitch motion. Here $\vec{n}=(n_1,n_2)$ is a unit normal vector in the $Ry$-plane directed into the body and $\vec{r}=(R,y)$ is the position vector on $S_0$ is the $Ry$-plane.

In the diffraction problem, the incident wave pot ential of unit wave amplitude is given as

$$\Phi_I=-\frac{g}{\sigma}e^{im_0x}\frac{\cosh m_0(y+h)}{\cosh m_0 h}, \tag{2.18}$$

where the wave is coming from $x=-\infty$ ($R=\infty$ and $\theta=\pi$). It is convenient to express $\exp(im_0x)$ in the above equation in terms of Bessel functions:

$$e^{im_0x}=\sum_{k=0}^{\infty}\varepsilon_k(i)^k J_k(m_0R)\cos k\theta, \tag{2.19}$$

where

$\varepsilon_k=1$ for $k=0$,

$\varepsilon_k=2$ for $k\ge 1$.

As in the case of the forced-motion problem, it is sufficient to solve for $k=0$ to obtain the vertical excitation force, and to solve for $k=1$ to obtain the surge and pitch excitation forces. It is customary to decompose to total potential into the known incident potential and the diffraction potential. Then for the diffraction potential, we simply specify the opposite normal velocity computed from the incident wave potential, on the body. By using (2.18) and(2.19), the normal velocity on the body for the $k$-th mode in the diffraction problem is given by

$$v_n^{(k)}=-\frac{\varepsilon_k(i)^k g}{\sigma\cosh m_0 h}\left[n_1\frac{dJ_k(m_0R)}{dR}\cosh m_0(y+h)+n_2 m_0 J_k(m_0R)\sinh m_0(y+h)\right] \tag{2.20}$$

on $S_0$, for $k=0,1,2,\cdots$.

In addition we have a new boundary condition along the y-axis ($R=0$) due to the reduction of the three-dimensional problem to sets of two-dimensional problems. This is

$$\varphi_n^{(k)}=0 \qquad \text{at } R=0,\ \text{when } k=0 \tag{2.21}$$

and

$$\varphi^{(k)}=0 \qquad \text{at } R=0,\ \text{when } k\ge 1 \tag{2.22}$$

## 3. Localized Finite-Element Method and Numerical Procedures

As mentioned earlier, the theory of the calculus of variations is used as the basis of the present numerical scheme. The equivalence to the solution of the original problem of the variational method for the functional associated with the original problem is discussed in earlier papers [1, 2, 3] by the present author.

Let us draw an imaginary line $J$ (a vertical circular cylinder in space) in the Ry-plane which separates the fluid into a region $D_1$, which encloses the body, and a region $D_2$ as shown in Figure 2. Then the original fluid domain $D$ is divided into two sub-domains, i.e., $D_1$ and $D_2$ with the common interface boundary $J$. The boundary of sub-domain $D_1$ is denoted $S_1=S_{F1}\cup S_0\cup y\cup S_{B1}\cup J$ and the boundary of the infinite sub-domain $D_2$ is denoted $S_2=J\cup S_{F2}\cup S_R\cup S_{B2}$. Let $\varphi_1$ and $\varphi_2$ denote the potentials in these sub-domains, respectively. Then we have

$$\begin{aligned}
&\frac{1}{R}\frac{\partial}{\partial R}(R\varphi_{1R})-\frac{k^2}{R^2}\varphi_1+\varphi_{1yy}=0 && \text{in } D_1\\
&\varphi_{1y}-v\varphi_1=0 && \text{on } S_{F1}\\
&\varphi_{1n}=v_n && \text{on } S_0\\
&\varphi_{1n}=0 && \text{on } S_{B1}\\
&\left.\begin{aligned}&\varphi_{1n}=0, \quad k=0\\ &\varphi_1=0 \quad k\geq 1\end{aligned}\right\} && \text{on } y\ (R=0)
\end{aligned} \tag{3.1}$$

and

$$\frac{1}{R}\frac{\partial}{\partial R}(R\varphi_{2R})-\frac{k^2}{R^2}\varphi^2+\varphi_{2yy}=0 \qquad \text{in } D_2$$

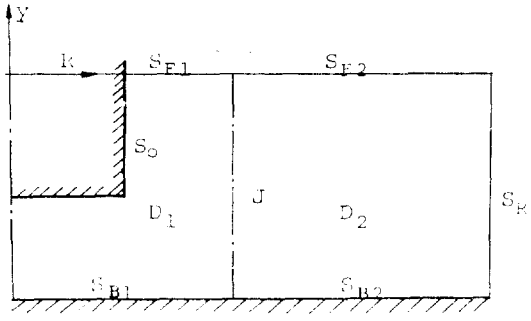


**Fig. 2** The Subdivision of the Localized Finite-Element Domain and Infinite Sub-Domain.

$$\begin{aligned}
&\varphi_{2y}-v\varphi_2=0 && \text{on } S_{F2}\\
&\varphi_{2n}=0 \text{ —} && \text{on } S_{B2}\\
&\lim_{R\to\infty}\sqrt{R}\,(\varphi_{2R}-im_0\varphi_2)=0 && (3.2)
\end{aligned}$$

In addition, we have

$$\varphi_1=\varphi_2 \text{ and } \varphi_{1n}+\varphi_{2n}=0 \qquad \text{on } J \tag{3.3}$$

where the normal vector is taken outwards from the fluid domain, for instance,

$$\varphi_{1n}=\varphi_{1R}, \quad \varphi_{2n}=-\varphi_{2R} \text{ on } J$$

The juncture conditions (3.3) imply that the potentials $\varphi_1$ and $\varphi_2$ have unique solutions.

Let us assume that the most general solution, or the solution space, of (3.2) is known and that $\varphi_2$ can be expressed in terms of the functions in the solution space with coefficients to be determined later. Then, by the approach given in Bai and Yeung [3] for the construction of the associated functionals for the above problem, the functionals are given by:

$$\begin{aligned}
F_1\{\varphi_1,\ \varphi_2\}=&\iint_{D1}\frac{1}{2}R\left(\varphi_{1R}^2+\varphi_{1y}^2+\frac{k^2}{R^2}\varphi_1^2\right)dRdy\\
&-\frac{v}{2}\int_{SF1}R\varphi_1^2\,ds-\int_{S0}v_n\varphi_1 ds\\
&+\int_J R(\varphi_1-\tfrac{1}{2}\varphi_2)\varphi_{2n}ds,
\end{aligned} \tag{3.4}$$

$$\begin{aligned}
F_2\{\varphi_1,\ \varphi_2\}=&\iint_{D1}\frac{1}{2}R\left(\varphi_{1R}^2+\varphi_{1y}^2+\frac{k^2}{R^2}\varphi_1^2\right)dRdy\\
&-\frac{v}{2}\int_{SF1}R\varphi_1^2\,ds-\int_{S0}v_n\varphi_1 ds\\
&+\int_J R[(\varphi_2-\varphi_1)\varphi_{1n}-\tfrac{1}{2}\varphi_2\varphi_{2n}]ds
\end{aligned} \tag{3.5}$$

Then, it may be shown that the solution of equations (3.1) to (3.3) is equivalent to the solution of

$$\delta F_1\{\varphi_1,\varphi_2\}=0, \tag{3.6}$$

or

$$\delta F_2\{\varphi_1,\varphi_2\}=0, \tag{3.7}$$

together with the essential condition (2.22) if $K\geq 1$.

In the numerical procedure, the trial function for $\varphi_1$ in $D_1$ is chosen from a simple polynomial function space, and the trial function for $\varphi_2$ in $D_2$ ($R\geq R_0$) is chosen from the solution space which satisfies (3.2). Here the solution space is constructed from the set of infinite discrete eigenfunctions. In order to numerically find the first variation of the functional, (3.4) or (3.5), which is zero, we simply require the first partial derivative of the functional with

respect to the undetermined coefficients of the trial functions to be zero, after the trial functions are substituted in the functional.This procedure reduces the functional equations to a set of linear algebraic equations. A procedure for treating an essential boundary condition in the functional is discussed in Bai.[2]

## 4. Numerical Results and Discussions

After the volocity potential has been obtained,the pressure can be computed by Bernoulli's equation

$$p=-\rho\Phi_t=R_e\{i\sigma\rho\varphi^{(k)}(R,y)\cos(k\theta)e^{-i\sigma t}\} \tag{4.1}$$

where the static pressure has been neglected. Then the added mass ($\mu$) and damping ($\lambda$) coefficients are defined as the integrals of the pressure along the body boundary as follows:

$$\mu_{11}+i\frac{\lambda_{11}}{\sigma}=\pi\rho\int_{S_0}R\varphi^{(1)}n_1ds \tag{4.2}$$

$$\mu_{16}+i\frac{\lambda_{16}}{\sigma}=\pi\rho\int_{S_0}R\varphi^{(1)}(r\times n)ds \tag{4.3}$$

$$\mu_{22}+i\frac{\lambda_{22}}{\sigma}=2\pi\rho\int_{S_0}R\varphi^{(0)}n_2ds \tag{4.4}$$

$$\mu_{66}+i\frac{\lambda_{66}}{\sigma}=\pi\rho\int_{S_0}R\varphi^{(1)}(r\times n)ds \tag{4.5}$$

$$\mu_{61}+i\frac{\lambda_{61}}{\sigma}=\pi\rho\int_{S_0}R\varphi^{(1)}n_1ds \tag{4.6}$$

where $\mu_{11}$ and $\lambda_{11}$ are the surge added-mass and damping coefficients and $\mu_{16}$ and $\lambda_{16}$ are the pitch added moment and damping coefficients both due to surge motion, $\mu_{22}$ and $\lambda_{22}$ are the heave added mass and damping coefficients due to heave motion, and $\mu_{61}$ and $\lambda_{61}$ are the surge added-mass and damping coefficients and $\mu_{66}$ and $\lambda_{66}$ are the pitch added-moment and damping coefficients both due to pitch motion. Here $\varphi^{(1)}$ in (4.2) and (4.3) is the potential for surge motion, and $\varphi^{(1)}$ in (4.5) and (4.6) is the potential for pitch motion.

The exciting forces can also be computed by

$$X=R_e\{(X_1+iX_2)e^{-i(\sigma t-\pi/2)}\} \tag{4.7}$$

$$Y=R_e\{(Y_1+iY_2)e^{-i(\sigma t-\pi/2)}\} \tag{4.8}$$

$$M=R_e\{(M_1+iM_2)e^{-i(\sigma t-\pi/2)}\} \tag{4.9}$$

where

$$X_1+iX_2=\pi\rho\sigma\int_{S_0}R\varphi^{(1)}n_1ds \tag{4.10}$$

$$Y_1+iY_2=2\pi\rho\sigma\int_{S_0}R\varphi^{(0)}n_2ds \tag{4.11}$$

$$M_1+iM_2=\pi\rho\sigma\int_{S_0}R\varphi^{(1)}(r\times n)ds \tag{4.12}$$

The potentials $\varphi^{(1)}$ in (4.10) and (4.12) are the same, and the potentials $\varphi^{(0)}$ and $\varphi^{(1)}$ in (4.10) through (4.12) are the total potentials, i.e.,the sum of the incident wave potential (of unit amplitude) and the corresponding diffraction potential of the same mode ($j=0$ or 1). The exciting forces and moment given in (4.10) through (4.12) can be expressed in a slightly different form, in terms of their magnitude and phase, i.e.,

$$X_1+iX_2=X_0e^{i\alpha_x},$$
$$Y_1+iY_2=Y_0e^{i\alpha_h},$$
$$M_1+iM_2=M_0e^{i\alpha_p}. \tag{4.13}$$

As mentioned earlier Newman [5] showed that the phase $\alpha_s$ of the horizontal excitation force is equal to the phase $\alpha_p$ of the pitch excitation moment.

### 4.1 A Submerged Half-Spheroid on the Bottom

In this sub-section a submerged half-spheroid lying on the bottom of a body of water of depth $h$ is considered, as shown in Figure 3. The equation of the spheroid is

$$\left(\frac{R}{a}\right)^2+\left(\frac{y}{c}\right)^2=1,\quad h/c=2.5,\quad a/c=2 \tag{4.14}$$

In the numerical computations, the localized finite-element domain was subdivided into 17 quadrilateral elements with a total of 72 nodes. The exciting forces and moment were computed for six different frequencies. These results are compared with those obtained by Rao and Garrison [4] in Table 1. In Figure 4 we only present the present numerical reuslts since the comparison is very good. The CPU computation time on an IBM 36CM 165 was about

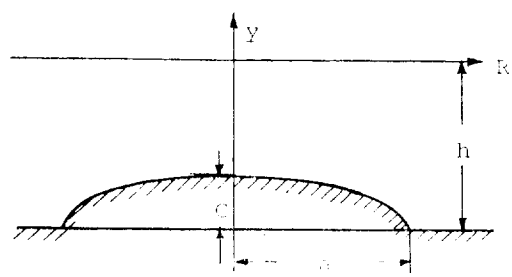


**Fig. 3** A Submerged Spheroid

**Table 1** The Excitation Forces and Moment on a submerged Half-Spheroid on the Bottom.(Here LFEM denotes the present method and R&G denotes Rao & Garrison). $\eta$ is the amplitude of the incident wave.

| $m_0a$ | $X_0/\rho ga^2\eta$ | | $Y_0/\rho ga^2\eta$ | | $M_0/\rho ga^3\eta$ | |
|---|---|---|---|---|---|---|
| | LFEM | R&G | LFEM | R&G | LFEM | R&G |
| 0.19 | 0.2589 | 0.2609 | 3.0500 | 3.1061 | 0.1464 | 0.1497 |
| 0.34 | 0.4356 | 0.4396 | 2.8660 | 2.9263 | 0.2471 | 0.2532 |
| 0.60 | 0.6348 | 0.63903 | 2.4010 | 2.4656 | 0.3613 | 0.3726 |
| 1.07 | 0.6532 | 0.6601 | 1.4910 | 1.5366 | 0.3886 | 0.3988 |
| 2.29 | 0.2174 | 0.2183 | 0.2703 | 0.2790 | 0.1576 | 0.1609 |
| 3.39 | 0.0404 | 0.0448 | 0.0403 | 0.0518 | 0.0455 | 0.0470 |

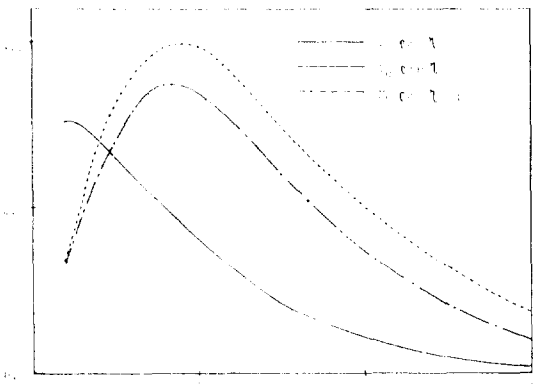

**Fig. 4** The Excitation Forces and Moment on a submerged Half-Spheroid on the Bottom. ($\eta$ is the amplitude of the incident wave)

1.9 seconds for each frequency.

### 4.2 Floating Axisymmetric Ocean Platforms

Four specific types of ocean platforms are treated in this sub-section. The sketches of each model are shown in Figure 5. Model Number 1 is a disc type, Model Number 2 consists of a disc with a long pipe. Model Number 3 is a spar type, and Model Number 4 is a modified disc type. All of the results for these models are given in Figure 6 through Figure 17 and in Table 2 through Table 4. For these models, all of the hydrodynamic coefficients are computed as well as the excitation forces and moment for ten frequencies; $\sigma=0.2$, 0.3, 0.4, 0.5, 0.6, 0.8, 1.0, 1.2, 1.6, and 2.0 (1/sec).

As mentioned earlier, there exists a symmetry relation between the off-diagonal added-mass and damping coefficients, i.e., the hydrodynamic coeffici-

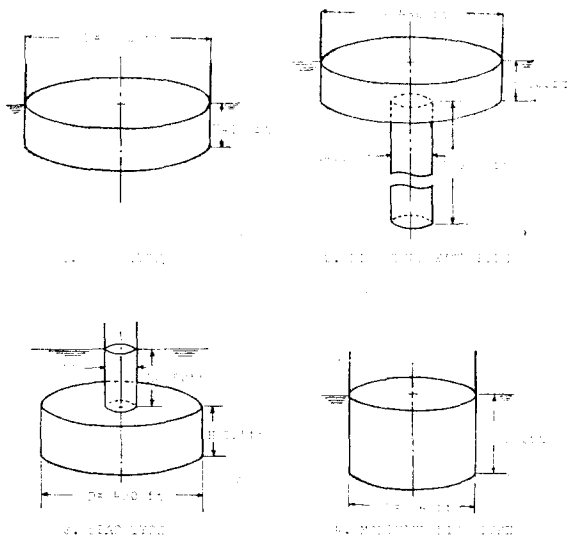

**Fig. 5** Dimensions of Axisymmetric Platforms

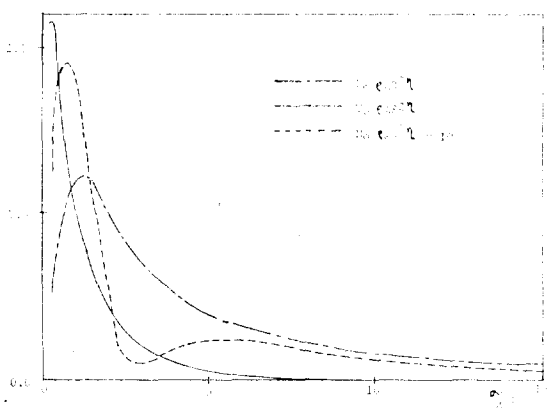

**Fig. 6** The Excitation Forces and Moment on the Model #1. (throughout following figures $R=\frac{D}{2}$)

**Table 2** The Hydrodynamic Coefficients of Model #1 due to Sway Motion in the 0.6 to 0.9 frequency range.

| $\sigma$ | $\mu_{11}/\rho$ | $\lambda_{11}/\rho\sigma$ | $\mu_{16}/\rho$ | $\lambda_{16}/\rho\sigma$ |
|---|---|---|---|---|
| 0.60000 | 1.822+6 | 5.450+6 | 8.375+7 | −1.882+7 |
| 0.64114 | 1.341+6 | 4.814+6 | 7.251+7 | 5.890+6 |
| 0.69813 | 9.565+5 | 3.997+6 | 5.095+7 | 2.567+7 |
| 0.76621 | 7.575+5 | 3.175+6 | 2.692+7 | 3.618+7 |
| 0.80000 | 7.465+5 | 2.801+6 | 1.481+7 | 3.780+7 |
| 0.84338 | 7.270+5 | 2.440+6 | 5.445+6 | 3.772+7 |
| 0.84908 | 7.301+5 | 2.393+6 | 4.125+6 | 3.757+7 |
| 0.85486 | 7.335+5 | 2.346+6 | 2.824+6 | 3.739+7 |
| 0.86071 | 7.380+5 | 2.300+6 | 1.544+6 | 3.717+7 |
| 0.86367 | 7.400+5 | 2.276+6 | 9.095+5 | 3.706+7 |
| 0.86665 | 7.425+5 | 2.253+6 | 2.818+5 | 3.693+7 |
| 0.86724 | 7.430+5 | 2.249+6 | 1.568+5 | 3.691+7 |
| 0.86784 | 7.435+5 | 2.244+6 | 3.209+4 | 3.688+7 |
| 0.86844 | 7.440+5 | 2.024+6 | −9.245+4 | 3.685+7 |
| 0.86904 | 7.445+5 | 2.235+6 | −2.167+5 | 3.683+7 |
| 0.87226 | 7.480+5 | 2.208+6 | −8.580+5 | 3.666+7 |
| 0.89760 | 7.745+5 | 2.028+6 | −5.695+6 | 3.534+7 |

ents computed from (4.3) and (4.6) are the same. However, our numerical results for $\mu_{16}$ and $\mu_{61}$ or $\lambda_{16}$ and $\lambda_{61}$ given in Table 4 are obtained independently. The agreements are good for all cases between $\mu_{16}$ and $\mu_{61}$, and $\lambda_{16}$ and $\lambda_{61}$.

For Model Number 1, the forced surge motion is treated for a wide range of frequencies in order to identify one of the approximate frequencies which gives $\mu_{16}=0$ when $\sigma\cong 0.868$ as shown in Table 2.

Table 3 shows the comparison of the heave added mass and damping coefficients for Model Number 2 with different and conditions on the attached long pipe. The results for the three different pipe-end conditions are very close to each other. These comparisons show that the hydrodynamic coefficients of heave motion of model Number 2 are insensitive to whether the pipe-end is closed, open, or infinitely long and open.

It is well known that the added mass of a circular cylinder of unit length, moving in a direction normal to its axis in an infinite fluid, is equal to the displaced mass of fluid. For example, a circular cylinder of radius 55 feet in Model Number 2 with unit length has an added mass of

$$\mu_{11}=\rho\pi(55)^2. \tag{4.15}$$

When we ignore the effect of the disc contribution to the added mass in Model Number 2, the added masses computed from only the long pipe section (2000 ft) becomes

$$\mu_{11}=\pi\rho(55)^2\cdot 2000\doteqdot(1.9\times 10^7)\rho \tag{4.16}$$

$$\mu_{16}=\mu_{61}=\pi\rho(55)^2\int_{-2100}^{-100} y\,dy\doteqdot(2.1\times 10^{10})\rho \tag{4.17}$$

$$\mu_{66}=\pi_f(55)^2\int_{-2100}^{-100} y^2\,dy\doteqdot(2.93\times 10^{13})\rho \tag{4.18}$$

It is of interest to note that comparison of the app roximate results given by (4.16) through (4.18) with the numerical solutions given in Figure 10 show good agreement. It is not surprising that the agreement is reasonable, since the major portion of Model Number 2 body is deeply submerged. In particular, the pitch added moment $\mu_{66}$ and its coupling added mass $\mu_{61}$ stay almost constant with respect to the different wave lengths, since the major contribution to these added masses comes from the deeply submerged part of the body.

It is also of interest to compare the results of Model Number 1 and of Model Number 2. The disc part of Model Number 2 has the same dimensions as Model Number 1 (see Figure 5). The sway added

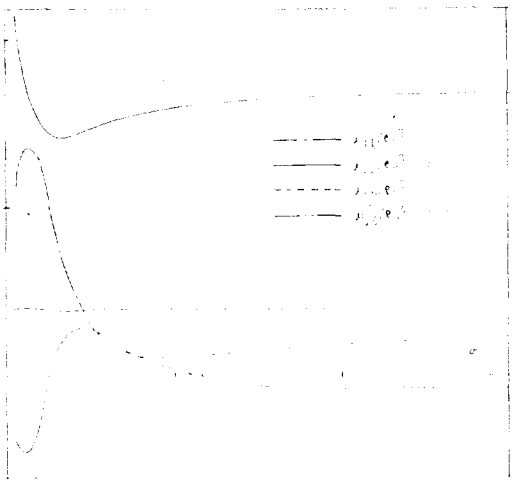

**Fig. 7** The Added Mass Coefficients of the Model #1.

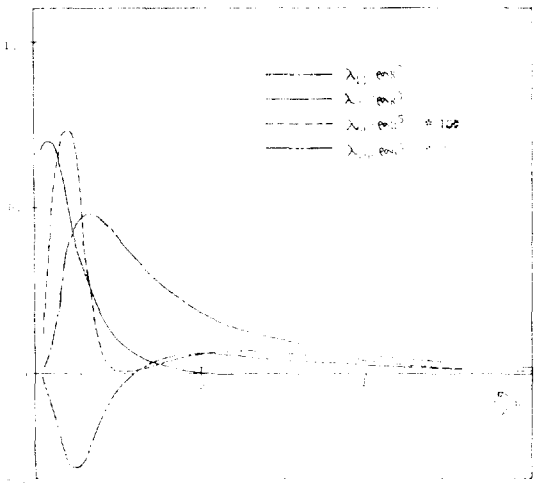

**Fig. 8** The Damping Coefficients of the Model # 1.

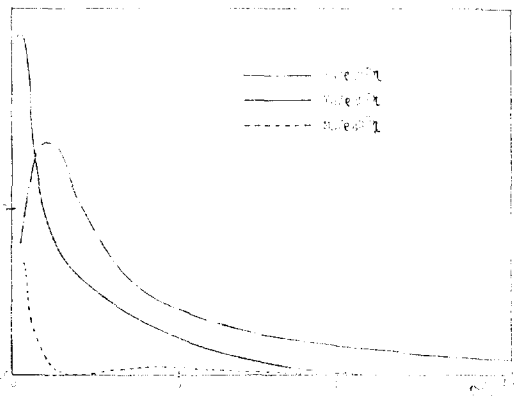

**Fig. 9** The Excitation Forces and Moment on the Model #2 with closed end.

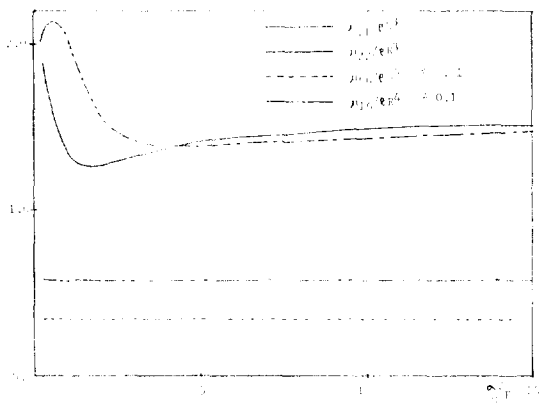

**Fig. 10** The Added Mass Coefficients of the Model #2 with closed end.

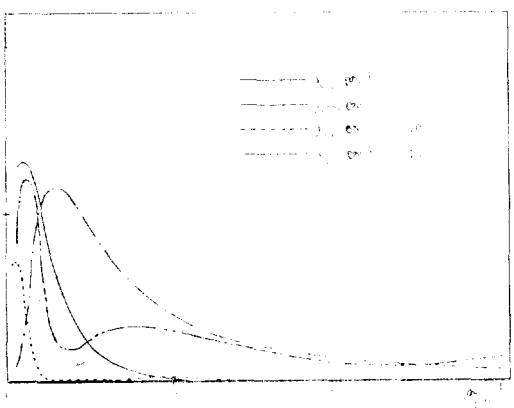

**Fig. 11** The Damping Coefficients of the Model # 2 with closed end.

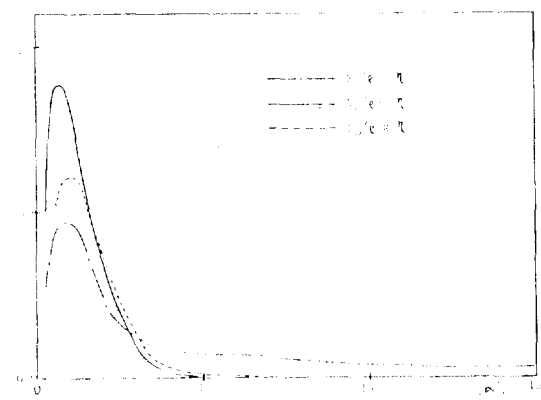

**Fig. 12** The Excitation Forces and Moment on the Model #3.

mass of Model Number 1 is approximately one order of magnitude less than that of Model Number 2, and the pitch added moment of Model Number 1 is approximately one percent of that of Model Number 2, as given in Figures 7, 8, 10, and 11. These comparisons show that neglect of the disc part of Model Number 2 is reasonable in equations (4.16) through (4.18). On the other hand, the heave added mass of Model Number 1 is very close to that of Model Number 2 Figures 7, 8, 10, and 11; this can be interpreted in the sense that the contribution of the attached pipe (with radius much smaller than that of disc) to the added mass is insignificant for most of the frequency range we tested. This result is also consistent with the comparisons of the heave added masses with three different end conditions on Model Number 2, given in Table 3.

The phase relations defined in (4.13) were also examined. It can be easily shown that the phase $\alpha_s$ of the horizontal excitation force is equal to the phase $\alpha_p$ of the pitch excitation moment, i.e., $\alpha_s=\alpha_p$ or $\alpha_s=\alpha_p+\pi$. A more detail tabulated results can be found in the author's earlier report [6]. The excitation forces computed by using the Haskind relations were compared with the results obtained by solving directly the diffraction problem. Agreement was good. However, the comparison is not included in the present report. A typical subdivision of these floating platform problems in the localized finite element method is 60 quadrilateral 8-node

**Table 3** The Heave Added Mass and Damping Coefficients of Model #2 with three different end conditions on the attached long pipe.

| $\sigma$ | Closed End | | Open End | | Infinitely Long & Open End | |
|---|---|---|---|---|---|---|
| | $\mu_{22}/\rho$ | $\lambda_{22}/\rho\sigma$ | $\mu_{22}/\rho$ | $\lambda_{22}/\rho\sigma$ | $\mu_{22}/\rho$ | $\lambda_{22}/\rho\sigma$ |
| 0.2 | 2.606+7 | 8.846+6 | 2.669+7 | 8.697+6 | 2.556+7 | 8.591+6 |
| 0.3 | 2.095+7 | 8.739+6 | 2.089+7 | 8.659+6 | 2.110+7 | 8.425+6 |
| 0.4 | 1.790+7 | 5.786+6 | 1.783+7 | 5.701+6 | 1.817+7 | 5.628+6 |
| 0.5 | 1.739+7 | 2.946+6 | 1.736+7 | 2.865+6 | 1.776+7 | 2.818+6 |
| 0.6 | 1.803+7 | 1.213+6 | 1.802+7 | 1.175+6 | 1.845+7 | 1.150+6 |
| 0.8 | 1.944+7 | 1.254+5 | 1.937+7 | 1.265+5 | 1.977+7 | 1.244+5 |
| 1.0 | 2.007+7 | 8.280+3 | 1.998+7 | 8.709+3 | 2.046+7 | 8.644+3 |
| 1.2 | 2.072+7 | 4.162+2 | 2.025+7 | 4.099+2 | 2.074+7 | 4.045+2 |
| 1.6 | 2.095+7 | 1.759+1 | 2.047+7 | 7.463−1 | 2.097+7 | 1.069+0 |
| 2.0 | 2.101+7 | 1.062+1 | — | — | 2.107+7 | 1.268−2 |

**Table 4** Added Mass and Damping Coefficients of Model #2 with closed End.

| $\sigma$ | $\mu_{16}/\rho$ | $\lambda_{16}/\rho\sigma$ | $\mu_{61}/\rho$ | $\lambda_{61}/\rho\sigma$ |
|---|---|---|---|---|
| 0.2 | 1.940+10 | 1.368+8 | 1.918+10 | 1.358+8 |
| 0.3 | 1.924+10 | 2.001+8 | 1.901+10 | 1.858+8 |
| 0.4 | 1.916+10 | 8.040+7 | 1.895+10 | 5.435+7 |
| 0.5 | 1.921+10 | 3.145+7 | 1.901+10 | 1.081+7 |
| 0.6 | 1.923+10 | 4.581+7 | 1.903+10 | 3.338+7 |
| 0.8 | 1.921+10 | 5.070+7 | 1.901+10 | 4.731+7 |
| 1.0 | 1.924+10 | 3.037+7 | 1.900+10 | 2.942+7 |
| 1.2 | 1.945+10 | 1.473+7 | 1.905+10 | 1.431+7 |
| 1.6 | 1.946+10 | 3.608+7 | 1.908+10 | 3.083+7 |
| 2.0 | 1.947+10 | 1.377+6 | 1.927+10 | 8.740+5 |

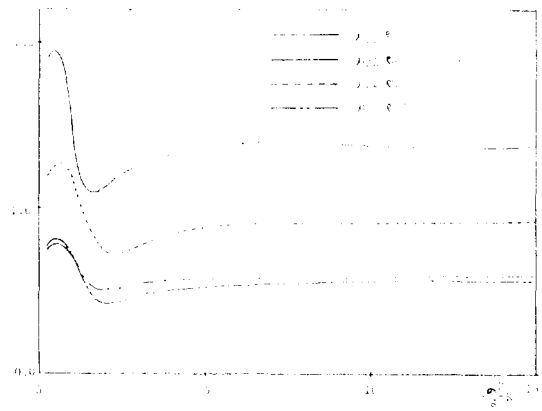

**Fig. 13** The Added Mass Coefficients of the Model #3.

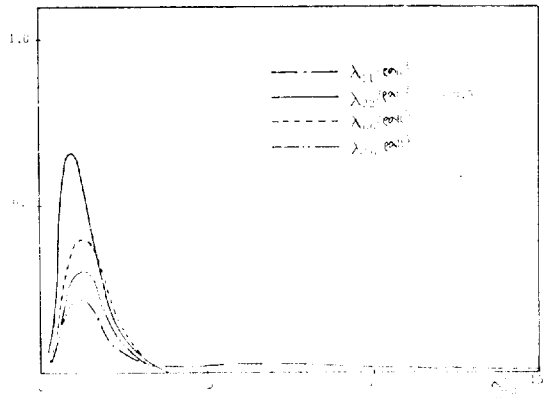

**Fig. 14** The Damping Coefficients of the Model #3.

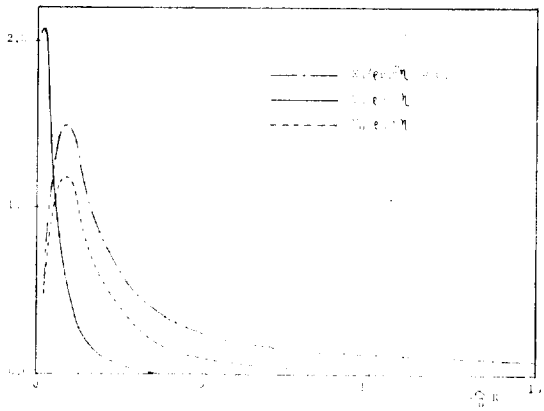

**Fig. 15** The Excitation Froces and Moment on Model #4.

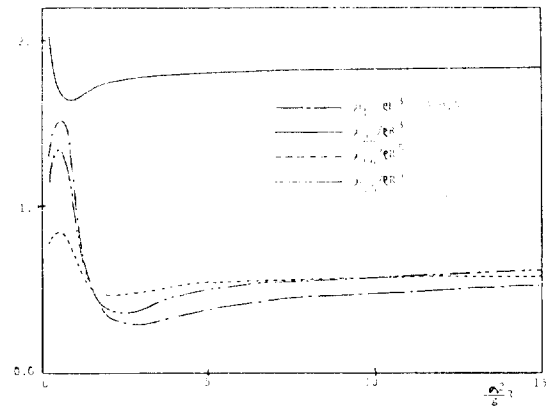

**Fig. 16** The Added Mass Coefficients of the Model #4.

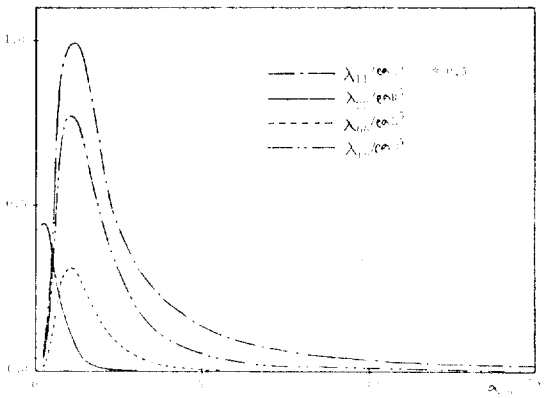

**Fig. 17** The Damping Coefficients of the Model #4.

elements with 217 total nodes. A typical computation CPU time on CDC 6700 was between 10 seconds and 25 seconds depending on the specific problem.

## REFERENCES


1. Bai, K.J., "A Varatiional Method in Potential Flows with a Free Surface," Ph.D. Dissertation, Department of Naval Architecture, University of California, Berkeley. 1972.
2. Bai, K.J., "A Localized Finite-Element Method for Steady, Two-Dimensional Free Surface Flow Problems, "The First International Conference on Numerical ship Hydrodynamics, Gaithersburg, Maryland, October 1975.
3. Bai, K.J. and Yeung, R.W., "Numerical Solutions to Free-Surface Flow Prow Problems. "The Tenth Symposium on Naval Hydrodynamics, Office of Naval Research, Cambridge, Mass., June 1974.
4. Rao, V.S. and Garrison, C.J., "Interaction of a Train of Regular Waves with a Rigid Submerged Spheroid," Journal of Ship Research, Vol. 20, No. 4, December 1976.
5. Newman, J.N., "The Interaction of Stationary Vessels with Regular Waves," The Eleventh Symposium on Naval Hydrodynamics, Office of Naval Research, London, England, 1976.
6. Bai, K.J., "The Added Mass and Damping Coefficients of and the Excitation Forces on Four Axisymmetric Ocean Platforms." David W. Taylor Naval Ship Research & Development Center, Bethesda, Maryland, Dept. Report, 1976.